Transactions of the 14th International Conference on Structural Mechanics in Reactor Technology (SMiRT 14), Lyon, France, August 17-22, 1997 BLDW/12

Strengths of dissimilar welded joints of 2 1/4 Cr-1Mo steel and Hastelloy XR

Muto Y.(1), **Hada K.**(2), **Sato K.**(3)
(1) Tokai Research Establishment, JAERI, Japan
(2) Japan Atomic Energy Research Institute, Japan
(3) Kawasaki Heavy Industries, Ltd., Japan

ABSTRACT

High temperature strengths of dissimilar TIG and EB welded joints of 2 1/4 Cr-1Mo steel and Hastelloy XR have been studied. Tensile tests, stress rupture tests and low cycle fatigue tests at 500℃ were carried out. The creep rupture strengths of TIG and EB welded joints were equivalent to that of 2 1/4Cr-1Mo steel. Fatigue strength of TIG welded joints was inferior to that of base metal. To examine the cause of premature failure, elastic-plastic stress analysis was carried out at the first cycle, cycles corresponding to 0.1 and 0.5 life times.

1. INTRODUCTION

Dissimilar welded joint of 2 1/4Cr-1Mo steel and Hastelloy XR is used in high temperature components for the high temperature gas-cooled reactor (HTGR). 2 1/4Cr-1Mo steel is a normalized and tempered one corresponding to ASTM SA 387 Grade 22 Class 2. Hastelloy XR is a Ni base heat resistant alloy which was modified from Hastelloy X to show good characteristics in the HTGR helium gas environment[1]. Two welding methods, that is, tungsten inert gas (TIG) arc welding and electron beam (EB) welding were employed. Hastelloy W was used as a material of the filler wire. Dissimilar welded joints between ferritic steel such as 2 1/4Cr-1Mo steel and Ni base alloy such as Hastelloy XR or austenitic stainless steel are widely used in thermal and nuclear power plants. As a result of vast previous research works[2,3,4], many features have been clarified regarding the strengths of such dissimilar welded joints. Nevertheless, some issues are still remained unsolved. In addition, there was no available data regarding creep and creep-fatigue strengths of the above welded joints. Then, tests have been carried out at 500℃ in the atmospheric environment.

The creep rupture strengths of welded joints were equivalent to that of 2 1/4Cr-1Mo steel, both in TIG and EB welded joints. However, the rupture elongation and reduction of area showed declining inclinations to a longer life time.

As for creep-fatigue tests, the strength of TIG welded joints was inferior to that of base metal, which means 2 1/4Cr-1Mo steel. On the other hand, the strength of EB welded joint was almost equivalent to that of base metal. 2 1/4Cr-1Mo steel and Hastelloy XR show contrary trends in a cyclic strength. The former shows a cyclic softening behavior while the latter shows a distinct cyclic hardening one. Regarding Hastelloy W, no cyclic data is available, but its behavior is thought to be similar to that of Hastelloy XR because they are essentially the same kind of material. Then, at the initial loading stages, strains at the portion of Hastelloy XR and Hastelloy W are larger than that of 2 1/4 Cr-1Mo steel. And, after less than 50 cycles, strain at the region of 2 1/4Cr-1Mo steel becomes larger. Stress analysis results showed that no effective stress concentration was generated in 2 1/4Cr-1Mo steel area at the vicinity of weld boundary except for initial loading cycles. Vickers hardness tests showed no softening to suggest decarburization at the above area. Therefore, the premature crack initiation at the bond of 2 1/4Cr-1Mo steel side is thought to be attributed to the complicated mixed effects due to both mechanical and metallurgical effects. Though the reason of reduction of fatigue strength of TIG welded joints was not clarified from the stress analysis, the direction of measured crack propagation coincided well with the ridges of stress and plastic strain contours.

2. TEST MATERIALS AND TESTING METHODS

Two plates with 15mm thickness were machined from the locations of a quarter of the thickness of 2 1/4Cr-1Mo steel block of W250mm×L475mm×T160mm. The material specification is in accordance with the ASTM standard SA387 Gr.22 Cl.2 and normalized and tempered material. Solution annealed Hastelloy XR rolled plate with 15mm thickness was used. Table 1 shows the chemical compositions of used materials.

Table 1 Chemical compositions of used materials

Hastelloy XR

C	Si	Mn	P	S	Ni	Cr	Co	Mo	W	Al	Ti	B	Fe	N
0.07	0.31	0.90	LAP	LAP	Bal.	21.67	<0.05	8.97	0.49	<0.05	<0.05	<0.001	18.31	0.006

LAP=low as practicable

2 1/4 Cr-1Mo steel

C	Si	Mn	P	S	Ni	Cr	Cu	Mo	Al	V	As	Sn	Co	Ti	Fe
0.14	0.08	0.54	LAP	LAP	0.12	2.36	0.09	1.04	0.018	<0.01	0.008	0.008	0.12	LAP	Bal.

Hastelloy W

C	Mn	Si	P	S	Cr	Mo	Fe	V	Co	Ni
0.01	0.61	0.34	<0.005	<0.005	5.05	24.51	5.27	0.32	<0.05	Bal.

Table 2 Welding conditions and configuration for the TIG welding

<table>
<tr><th rowspan="3">Joint configuration</th><th rowspan="3">Built-up sequence</th><th colspan="7">Welding conditions</th></tr>
<tr><th rowspan="2">Pass</th><th rowspan="2">Dia. of filler metal</th><th rowspan="2">Welding current</th><th rowspan="2">Arc voltage</th><th rowspan="2">Welding speed</th><th colspan="2">Shield gas flow</th></tr>
<tr><th>Torch</th><th>Back-up</th></tr>
<tr><td rowspan="2">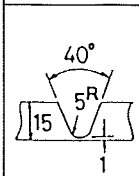</td><td rowspan="2">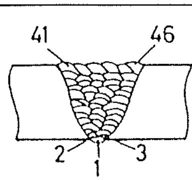</td><td>1 - 3</td><td>1.2 mm</td><td>60 - 70A</td><td>7 - 8V</td><td rowspan="2">50 - 60 mm/min</td><td rowspan="2">6 l/min</td><td>10 l/min</td></tr>
<tr><td>4 - 46</td><td>1.2 mm</td><td>70 - 80A</td><td>8 - 9V</td><td></td></tr>
</table>

The welding conditions of TIG welding were an electric current of 60 to 80A, voltage of 7 to 9V and welding velocity of 50 to 60 mm/min. U type edge configuration was used. Number of passes was 46. Those of EB welding were an electric current of 40mA, voltage of 225kV and a beam velocity of 200mm/min. After the welding and radiography inspection, the plate was annealed at temperature of 700±20℃ for one hour for the stress release.Tables 2 and 3 show the welding conditions and configurations for the TIG and EB welding, respectively.

Table 3 Electron beam welding conditions

Joint configurations	Welding conditions					
	Pitch (Torr)	D_F (mm)	a_b (mm)	I_b (mA)	V_b (kV)	v_b' (mm/min)
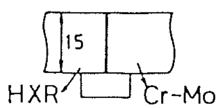	5×10^{-4}	175	1.28	40	225	200

Tensile and creep specimens have 6mm diameter and 30mm gauge length. The welded section was adjusted to locate at the central portion of specimen in the axial direction. A configuration of fatigue specimens is an hour glass type shown in Fig.1. The interface section between Hastelloy W weld metal and 2 1/4Cr-1Mo steel was adjusted to locate at the center of specimen, because a fracture was predicted to occur at this section. The minimum diameter was 8mm and the curvature radius was 48mm.

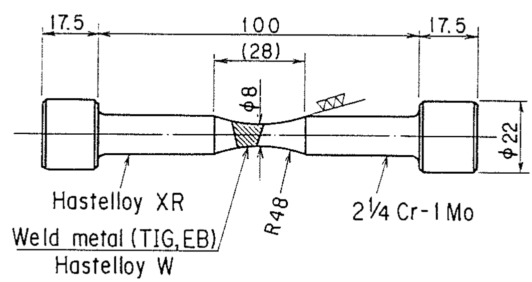

Fig. 1. Fatigue test specimen

The method of tensile test was based on the Japan Industrial Standard which means a strain rate of 0.3%/min to 0.2% yield stress and thereafter 8.3%/min. Creep tests were carried out using the lever type machines in the air environment. Fatigue tests were using a survo-controlled fatigue test machine and by Induction heating in the atmospheric environment. By contacting quartz sticks side by side on the specimen at the location of 2 1/4Cr-1Mo steel which is apart by 0.5 to 1mm from the bond, a diametric strain ε_d was measured. Then, the axial strain ε was controlled in accordance with the following equation[2]:

$$\varepsilon = \frac{\sigma}{E}(1-2\nu)-2\varepsilon_d \qquad (1)$$

where σ = stress (MPa)

E = elastic modulus (MPa)

ν = Poisson's ratio

Triangular waveform was mainly employed while trapezoidal waveform of 10min tensile hold time was also used. All fatigue tests were strain controlled and had a strain rate of 0.1%/s.

3. TEST RESULTS

3.1 *Tensile tests*

Figure 2 shows the test results. In this series of tests, tensile tests at 500℃ for the Hastelloy XR was not carried out. Then, data at 600℃ of another series of tests machined from another charge was used. In the case of Hastelloy XR, a yield stress and tensile strength at 600℃ are almost the same as those at 500℃ (the difference is less than 10%). The yield strength of Hastelloy W is predicted to be 260 MPa from the reference[6]. 2 1/4Cr-1Mo steel is harder than both Hastelloy XR and Hastelloy W.

The deformation curves for TIG welded joints and EB welded joints come to the intermediate region between 2 1/4Cr-1Mo steel and Hastelloy XR. The curve of EB joints comes below that of TIG joints, because Hastelloy XR is softer than Hastelloy W. Tensile strength of both the welded joints are equivalent to that of 2 1/4Cr-1Mo steel because all the ruptures occurred at the 2 1/4Cr-1Mo steel section. The rupture elongation for 2 1/4Cr-1Mo steel and Hastelloy XR were 20.5～22.0% and 53.8%, respectively and the reduction of area were 75.0%～75.8% and 47.5%, respectively. The rupture elongation and reduction of area for the welded joints (TIG and EB) were 15.4～22.3% and 61.0～72.6%, respectively. The values were similar to those for the 2 1/4Cr-1Mo steel.

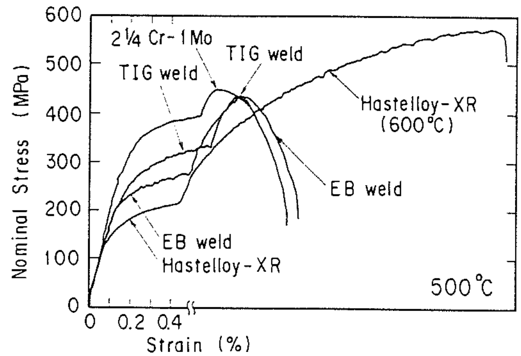

Fig. 2 Stress-strain curves for the test materials

3.2 *Stress-Rupture Tests*

Figure 3 shows dependence of time to rupture on the initial stress. The creep rupture strengths of TIG and EB welded joints were equivalent to those of 2 1/4Cr-1Mo steel. In the case of TIG welded joints, at lower stress, the rupture occurred at the area of welding interface (bond) of 2 1/4Cr-1Mo side while the rupture occurred at 2 1/4Cr-1Mo area at higher stress. The weld metal of Hastelloy W deformed very little. Therefore, the reductions of area for TIG welded joints at lower stress were observed to be significantly reduced as shown in Fig.4. On the other hand, rupture elongation for them were about 10%, which were only a little smaller than those for both the 2 1/4Cr-1Mo steel and EB welded joints.

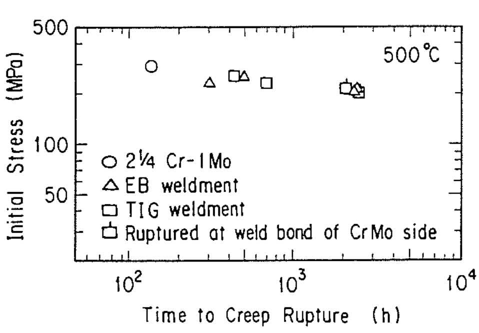

Fig.3 Time to creep rupture.

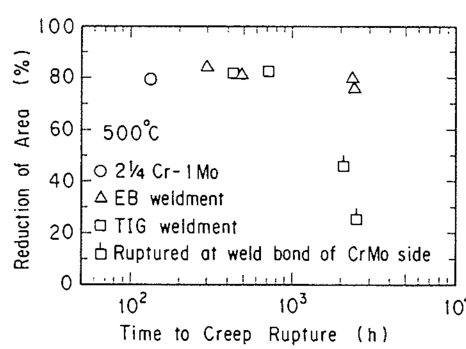

Fig.4 Reduction of area

Figure 5 shows a microstructure of stress-ruptured specimen of TIG welded joint. It can be seen that a crack was initiated at the weld bond (A) and propagated through 2 1/4Cr-1Mo steel at the vicinity of bond, and resulted in rupture. The opposite side bond (B) was also observed to be peeled off a little.

3.3 *Fatigue tests*

3.3.1 *Fatigue life*

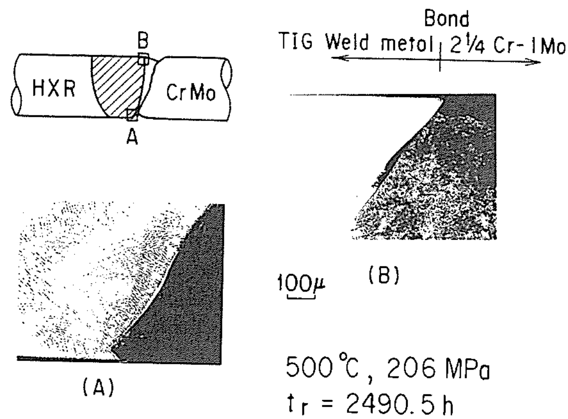

Fig. 5 Microstructure of creep-ruptured TIG specimen

Figures 6 and 7 show the cycles to failure dependent on the total strain range and plastic strain range, respectively.

From these figures, the following are known.

1) In the case of 2 1/4Cr-1Mo steel, the relationships between plastic strain range and cycles to failure and also between an elastic strain range and cycles to failure are well correlated by straight lines. The values of fatigue life are roughly equivalent to the previous results obtained for the annealed material (AN)[7] and normalized tempered (NT) material[8].

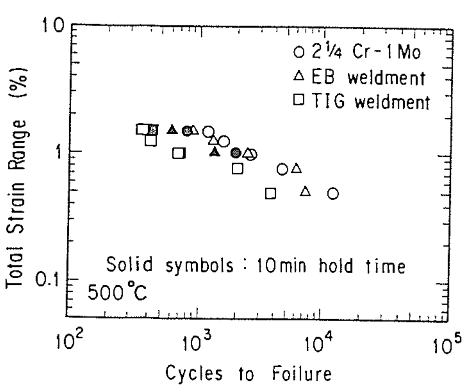

Fig.6 Total strain range versus cycles to failure

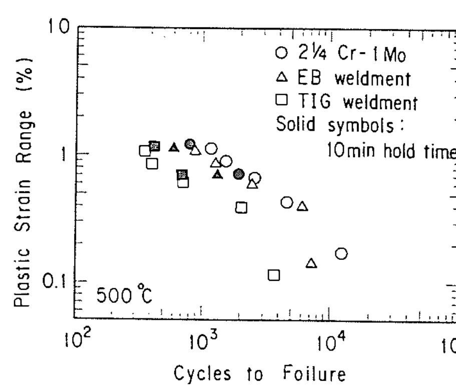

Fig.7 Plastic strain range versus cycles to failure

2) Fatigue life of EB welded joints is equivalent to that of 2 1/4Cr-1Mo steel.

3) On the other hand, that of TIG welded joint is inferior to them and becomes 1/3 of the base metal. Here, the relationship between the elastic strain range and cycles to failure does not change from that of base metal while the relationship between the plastic strain range and cycles to failure is different from that of base metal.

4) In the relationship between the plastic strain range and cycles to failure, the data are well correlated by straight lines in the higher stress regime. However, the trends of these data begin to decline rapidly in the lower stress regime.

5) The crack originates at the 2 1/4Cr-1Mo steel of weld bond for both the EB and TIG welded joints.

6) By introducing hold time of 10 minutes, the fatigue lives of 2 1/4Cr-1Mo steel and EB welded

joints decrease a little while no influence was observed in the TIG welded joints.

3.3.2 *Cyclic stress-strain behavior*

Figure 8 shows the cyclic stress-strain curves. 2 1/4Cr-1Mo steel shows cyclic softening behavior. On the contrary, Hastelloy XR shows a distinct cyclic hardening behavior.

As the strain hardening of Hastelloy XR is so rapid that the relation between strengths of these materials reverses less than 50 cycles, which is only about 1/20 of total cycles to failure. The behavior of TIG and EB welded joints are similar to that of 2 1/4Cr-1Mo steel. The values at the initial stage are thought to be attributed to the higher strength of Hastelloy W, though the strength of Hastelloy W is not known exactly. The softening behavior are necessarily attributed to that of 2 1/4Cr-1Mo steel.

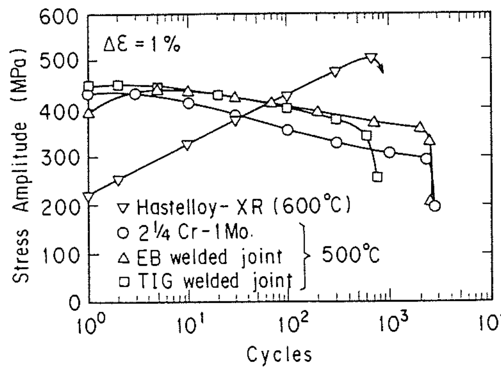

Fig.8 Cyclic stress-strain curves

3.3.3 *Microstructure of failed specimen*

The photo of microstructure for the TIG welded joints with 10 mm hold time is shown in Fig.9. Almost the same behavior can be seen for the triangular waveforms of TIG welded joints and also EB welded joints. Crack started at the weld bond (It was initiated at the 2 1/4Cr-1Mo steel region at the vicinity of weld bond in some cases). Then, it propagated to the direction declining by 20 - 40 degrees against the loading axis.

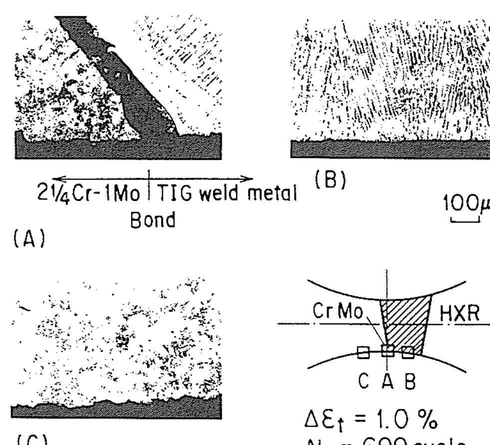

Fig.9 Microstructure of fatigue-failed specimen

4. STRESS ANALYSIS

As the mechanical properties of 2 1/4Cr-1Mo steel and Hastelloy W are different and moreover, their relative strengths change, that is, that of 2 1/4Cr-1Mo steel is higher than that of Hastelloy W at the first loading cycles, and after less than 50 cycles, the relation is reversed. Therefore, some stress concentration will be induced at the vicinity of interface and it will become cycle dependent. To clarify them, finite element stress analysis was carried out. For the simplification, uniform specimen model was employed instead of the hour glass specimen.

From Fig.8, the first, 72th and 358th cycles of $\Delta\varepsilon$=1.0% were selected for the calculation. They correspond to the initial loading, 0.1 and 0.5 time points of total life, respectively. Stress amplitudes for the fatigue test of TIG welded joint in the $\Delta\varepsilon$=1.0% were known, to be 412, 373 and 340 MPa, respectively. An axial load was imposed up to these values monotonically and stress and strain distributions were calculated.

The computer code "ABAQUS" was used for the analysis. A bilinear stress-strain relationship was made and used based on both the monotonic and cyclic curve for each material. The material properties used for the analysis are shown in Table 3. The contours of von Mises effective stress and equivalent plastic strain in the near-boundary area are given in Fig. 10.

Table 3 Mechanical properties used for the stress analysis

Materials		2 1/4Cr - 1Mo steel			Hastelloy XR and W		
Cycle	N	1	72	358	1	72	358
ν		0.3			0.3		
E	MPa	1.75×10^5			1.61×10^5		
H	MPa	0.767			3.05		
σ_y	MPa	379.2	313.5	279	200.0	327.6	416.7

As cracks have been initiated at the edge of 2 1/4Cr-1Mo steel side of the weld boundary and propagated through 2 1/4Cr-1Mo steel, the stress and strain behaviors in 2 1/4Cr-1Mo steel area are examined first.

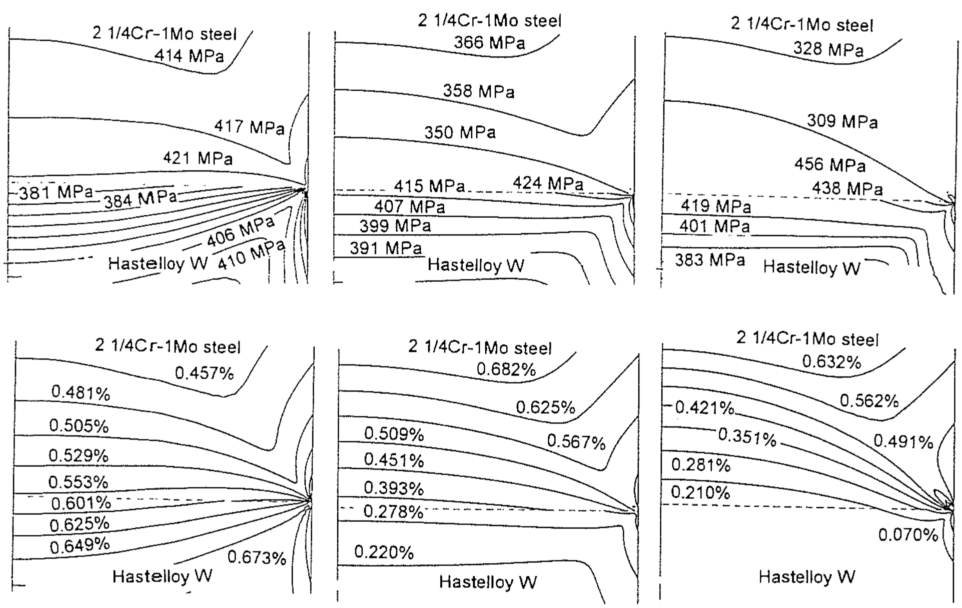

Axial load = 412 Mpa N=1st | 373 Mpa N=72th | 340 Mpa N=358th

Fig. 10. Von Mises effective stress and equivalent plastic strain at the vicinity of weld boundary for the cycles = 1st, 72th and 358th (R-z plane, R=0 to R_o)

At the initial loading cycle, the value of effective stress at the boundary is 421 MPa, which is a little higher than the average axial stress value of 412 MPa. This increase is caused by a radial compressive stress generated there. A small plastic strain concentration is observed corresponding to the stress. In 72th cycle, the stress concentration and then plastic strain concentration have disappeared since the relative hardness values between 2 1/4Cr-1Mo steel and Hastelloy W have been reversed. The values of stress and plastic strain at the boundary are rather smaller than those at the area apart from the boundary. Therefore, it cannot be explained why the fatigue strength of TIG welded joints have decreased.

The stress and plastic strain distributions are worthy of note. The ridge of contour (stress and plastic strain extremes) shows an inclined line against both the loading axis and weld boundary, The inclined angle is about 45° and coincide well with that of measured crack propagation.

As for the stress and plastic strain distributions in the Hastelloy W area, distinct stress concentration is observed at the edge of the boundary both in 72th and 358th cycles. This is attributed to the radial compressive stress. However, the amount of corresponding plastic strain is very small because of Hastelloy W's large plastic hardening coefficient (H).

5. SUMMARY

As a result of tensile, stress-rupture and low-cycle fatigue tests and also FEM stress analysis, the following are clarified for the dissimilar TIG and EB welded joints between 2 1/4Cr-1Mo steel and Hastelloy XR.

1) In tensile tests, both TIG and EB welded joints fractured at 2 1/4 Cr-1Mo region. The tensile strengths were equivalent to that of 2 1/4Cr-1Mo steel.

2) In stress-rupture tests, the strengths of both TIG and EB welded joints were equivalent to those of 2 1/4Cr-1Mo steel. In the case of TIG welded joints, however, brittle decohesion rupture was observed as the stress becomes lower,

3) In low cycle fatigue tests, the strength of TIG welded joints became lower than that of base metals, though the strength of EB welded joints were equivalent to that of base metal.

4) Introducing 10 min hold time, the fatigue strengths of both 2 1/4Cr-1Mo steel and EB welded joints decreased.

5) 2 1/4Cr-1Mo steel shows a cyclic softening behavior. On the other hand, Hastelloy XR shows distinct cyclic hardening behavior. The behavior of Hastelloy W is thought to be similar to that of Hastelloy W.

6) FEM stress analysis showed no effective stress concentration at 2 1/4Cr-1Mo area adjacent to the weld bond. However, the ridge of stress and strain contours coincided well with the direction of measured crack propagation.

7) The cause of life reduction for the TIG welded joints in the low cycle fatigue tests is still not clear because no effective stress concentration was calculated and no metallurgical deterioration was observed from the measurement of hardness.

REFERENCS

1. Tanaka,R. & T.Kondo 1984. *Nuclear Technology* 66: 75-87.
2. Lundin,C.D. 1982 *Welding Journal* 61,No.2: 58-s-63-s.
3. Setoguch,K. et al. Proc. ASME Int. Conf. on Advances in Life Prediction Method, New York, April 18-20, 1983: 179-185.
4. Roberts,D.I. et al. 1985 *J. Pressure Vessl Technology* 107: 247-254.
5. ASTM 1995. Annual Books of ASTM Standards 03.01, E-606: 525-539.
6. Mitsubishi Matrrials Co. 1984. Private communications.
7. Brinkman,C.R. 1976 *J. of Nuclear Materials* 62: 181-204.
8. Kodaira,T. et al. 1985 JAERI-M 85-170 (In Japanese).